CPC(HEP & NP), 2009, **33**(1): 31—35 Chinese Physics C Vol. 33, No. 1, Jan., 2009

Theoretical calculation of kerma coefficients for n+^{16}O reaction below 30 MeV*

QU Wen-Jing(渠文静) LIU Ji-Feng(柳继锋) SUN Xiao-Jun(孙小军)[1)]

(College of Physics and Electronic Engineering, Guangxi Normal University, Guilin 541004, China)

Abstract On the basis of the light nuclear reaction model, a new kerma coefficient formula has been developed. In terms of the analysis for n+^{16}O reactions below 30 MeV, the average energies of all kinds of the emitted particles are presented. The calculated partial kerma coefficients agree well with the existing experimental data. The discrepancies of the total kerma coefficients between the calculation and the measurement are analyzed in detail.

Key words kerma coefficient, light nucleus reaction model, energy balance

PACS 24.10.-i, 25.40.-h, 28.20.-v

1 Introduction

Reactions of fast neutrons with a light nucleus that lead to heating due to charged particles and the recoil nucleus have great importance in the prediction and analysis of the thermomechanical performance, in radiation shielding, in therapy beams and so on. The key response function for heating is the kerma coefficients[1]. The acronym kerma stands for kinetic energy released in matter. Usually, kerma coefficients are evaluated by nuclear data processing codes, such as NJOY[2] and MAZE[3], which are based on the nuclear data library. However, the emitted charged-particle information of neutron induced light nucleus reactions below 20 MeV is incomplete in libraries, such as ENDF/B-VIIb3, JENDL-3.3 etc and their earlier versions. For example, the outgoing neutron double-differential cross sections of oxygen from ENDF/B-VIIb3 were only determined by an isotropic method, and the same data from JENDL-3.3 are absent. Therefore, the kerma coefficients derived from the nuclear data library are inaccurate. Actually, for the neutron induced light nucleus reactions, all of the residual states are discrete levels, so the secondary particle emissions are all between these discrete levels, belonging to the sequential emissions or out-of-order emissions. Therefore, the energies for all kinds of the secondary particles are different. This reaction mechanism is so complex that the theoretical description is not well settled in the world. Fortunately, the nuclear reaction model for neutron induced light nucleus reaction is available[4]. The key point of this model is that the conservation of energy, angular momentum and parity in the emissions from a compound nucleus to the discrete levels of the residual nuclei with pre-equilibrium mechanism is taken into account properly. The total outgoing neutron energy-angular spectra for ^{6}Li[5], ^{7}Li[6], ^{10}B[7], ^{11}B[8], ^{12}C[9], ^{14}N[10], ^{16}O[11] and ^{19}F[12] have been successfully calculated by this model in earlier works. These results agree fairly well with the experimental data.

In this paper, on the basis of this light nucleus reaction model, we determine a new kerma coefficient formula and present the average energies of the emitted particles in each channel of the n+^{16}O reaction, keeping energy conservation strictly. The calculated partial kerma coefficients agree well with the existing experimental data. The discrepancies of the total kerma coefficients between the calculation and the measurement are analyzed in detail.

2 Kerma coefficient formula and the average energy of the emitted particles

According to the light nucleus reaction model, the

Received 24 June 2008

* Supported by National Natural Science Foundation of China (10547005)

1) E-mail: sxj0212@mailbox.gxnu.edu.cn

total kerma coefficient is given by

$$K_{\rm tot}=\sum_i K_i = N\sum_{ijk}\overline{E}_{ijk}(E_{\rm n})\sigma_{ijk}(E_{\rm n}), \qquad (1)$$

where $K_{\rm tot}$ is the total kerma coefficient expressed in fGy·m^2, and K_i is the partial kerma coefficient of the i-th typical charged-particle (including the recoil nucleus). In the laboratory system, $\overline{E}_{ijk}(E_{\rm n})$ and $\sigma_{ijk}(E_{\rm n})$ are the average energy (expressed in MeV) and production cross section (expressed in barn) respectively, which are dependent on the incident neutron energy $E_{\rm n}$. Here, j denotes the type of reaction channel and k characterizes the excitation energy level of the residual nucleus which can emit secondary particles, or proceed via two-body separation, or decay by gamma ray emission. The coefficient, $N=9.64853/M_{\rm A}$, converts the unit of the kerma coefficient from MeV·b to fGy·m^2, where $M_{\rm A}$ is the target nucleus mass in units of u. For the n+^{16}O reaction, N is 0.603033.

For incident neutron energies below 30 MeV, the accessible reaction channels theoretically are more than 50 in the n+^{16}O reaction. However, because of the higher thresholds and Coulomb barrier, the cross sections of some channels are too small to be detected in practice. The binding energies (B), the reaction Q values and threshold energies ($E_{\rm th}$) comprise all the information on the n+^{16}O reaction channels considered in this paper and are listed in Table 1, for an incident neutron energy $E_{\rm n}$ up to 30 MeV.

Table 1. The accessible reaction channels, binding energy (B), Q value and threshold energy ($E_{\rm th}$) for n+^{16}O reaction at $E_{\rm n}\leqslant$30 MeV. The unit of B, Q and $E_{\rm th}$ is MeV.

No.	channel	B	Q	$E_{\rm th}$
1	(n,γ)	0.000	4.143	0.000
2	(n,n)	4.143	0.000	4.439
3	(n,p)	13.780	−9.637	10.2447
4	(n,α)	6.358	−2.215	2.3547
5	(n,d)	14.046	−9.9030	10.5275
6	(n,t)	18.622	−14.4790	15.3920
7	(n,^{3}He)	18.760	−14.6170	15.5387
8	(n,^{5}He)	12.199	−8.0560	8.5640
9	(n,^{6}Li)	23.5614	−19.419	20.6436
10	(n,2n)	15.663	−15.6630	16.6507
11	(n,np)	12.127	−12.1270	12.8917
12	(n,nα)	7.161	−7.1610	7.6126
13	(n,nd)	20.736	−20.7360	22.0436
14	(n,pn)	2.490	−12.1270	12.8917
15	(n,αn)	4.946	−7.1610	7.6126
16	(n,2α)	10.646	−12.8610	13.6720
17	(n,dn)	10.833	−20.7360	22.0436
18	(n,2np)	7.297	−22.9599	24.4078
19	(n,npn)	10.833	−22.9599	24.4078
20	(n,p2n)	10.833	−22.9599	24.4078
21	(n,2αn)	1.665	−14.5257	15.4417

The 1st to 9th reaction channels single particle are emitted, the others pertain to the composite particles emission processes. The considered reaction mechanism of the n+^{16}O reaction includes first particle emission, second particle emission, the third particle emission from the residual nucleus discrete levels and the motion of the residual nuclei via two-body separation after the third particle has been emitted, usually not considered in other references. The average emitted energies of the first particle and the second particle are given in the formulae (43)—(52) in Ref. [4]. However n+^{12}C reaction lacks the processes of the third particle emission and the two-body separation from the corresponding residual nuclei. In this paper we complementarily give the energy expressions of these processes, such as the 18th to 20th channels.

In CMS (center-of-mass system), the energies carried by the third emitted particle and its residual nucleus are given by

$$\overline{E}^{m_3}_{c,k_3}=\frac{M_3}{M_2}(E_{k_2}-B_3-E_{k_3})+\frac{m_3}{M_2}E^{M_2}_{c,k_2}\ , \qquad (2)$$

and

$$\overline{E}^{M_3}_{c,k_3}=\frac{m_3}{M_2}(E_{k_2}-B_3-E_{k_3})+\frac{M_3}{M_2}E^{M_2}_{c,k_2}\ . \qquad (3)$$

In the laboratory system they attain the following forms

$$\overline{E}^{m_3}_{l,k_3} = \frac{m_0m_3}{M_0^2}E_{\rm n}+\frac{M_3}{M_2}(E_{k_2}-B_3-E_{k_3})+\frac{m_3}{M_2}E^{M_2}_{c,k_2}- \frac{2m_3}{M_0M_1}\sqrt{m_0M_1E_{\rm n}E^{M_1}_{c,k_1}}f^{m_1}_1(c)\ , \qquad (4)$$

and

$$\overline{E}^{M_3}_{l,k_3} = \frac{m_0M_3}{M_0^2}E_{\rm n}+\frac{m_3}{M_2}(E_{k_2}-B_3-E_{k_3})+\frac{M_3}{M_2}E^{M_2}_{c,k_2}- \frac{2M_3}{M_0M_1}\sqrt{m_0M_1E_{\rm n}E^{M_1}_{c,k_1}}f^{m_1}_1(c)\ . \qquad (5)$$

The physical quantities used in this paper are defined as in Ref. [4]. If the reaction channel ends by gamma decay, then E_{k_3} is the gamma decay energy. Therefore, the total released energy reads as follows

$$\overline{E}^T_l = \overline{E}^{m_1}_{l,k_1}+\overline{E}^{m_2}_{l,k_2}+\overline{E}^{m_3}_{l,k_3}+\overline{E}^{M_3}_{l,k_3}+E_{k_3}= E_{\rm n}+B_0-B_1-B_2-B_3. \qquad (6)$$

Obviously, the energy balance is strictly fulfilled.

However, in the case of the (n, 2αn) channel, the residual nuclei ^{8}Be, which is an unstable nucleus, proceeds via two-body separation at the state of E_{k_3} level after the third particle being emitted. Here, the energies carried by two clusters in the CMS can also be obtained by

$$\overline{E}^{m_4}_{c,k_4}=\frac{M_4}{M_3}(Q_{b4}+E_{k_3})+\frac{m_4}{M_3}\overline{E}^{M_3}_{c,k_3}\ , \qquad (7)$$

and

$$\overline{E}^{M_4}_{c,k_4} = \frac{m_4}{M_3}(Q_{b4}+E_{k_3}) + \frac{M_4}{M_3}\overline{E}^{M_3}_{c,k_3} \ . \tag{8}$$

In the laboratory system, they become

$$\begin{aligned}\overline{E}^{m_4}_{l,k_4} &= \frac{m_0 m_4}{M_0^2}E_{\rm n} + \overline{E}^{m_4}_{c,k_4} - \\ &\frac{2m_4}{M_0 M_1}\sqrt{m_0 M_1 E_{\rm n} E^{M_1}_{c,k_1}}\, f_1^{m_1}(c) \ ,\end{aligned} \tag{9}$$

and

$$\begin{aligned}\overline{E}^{M_4}_{l,k_4} &= \frac{m_0 M_4}{M_0^2}E_{\rm n} + \overline{E}^{M_4}_{c,k_4} - \\ &\frac{2M_4}{M_0 M_1}\sqrt{m_0 M_1 E_{\rm n} E^{M_1}_{c,k_1}}\, f_1^{m_1}(c) \ .\end{aligned} \tag{10}$$

Therefore, the total released energy reads as follows

$$\begin{aligned}\overline{E}^{T}_{l} &= \overline{E}^{m_1}_{l,k_1} + \overline{E}^{m_2}_{l,k_2} + \overline{E}^{m_3}_{l,k_3} + \overline{E}^{m_4}_{l,k_4} + E^{M_4}_{l,k_4} = \\ &E_{\rm n} + B_0 - B_1 - B_2 - B_3 + Q_{b4},\end{aligned} \tag{11}$$

where the Q_{b4} is the reaction Q value of the two cluster separation, and the energy balance is still fulfilled.

For nonelastic processes of neutron-induced reaction, the LUNF code[4] was used to calculate the cross sections of different channels, angular distributions and the double-differential cross sections. This code treats neutron-induced reaction as proceeding through an initial pre-equilibrium emission mechanism between discrete levels, followed by a process of sequential particle emission from decaying compound nuclei, until the final residual nucleus attaining its ground state via gamma-ray emission. The unified Hauser-Feshbach and exciton model theory is used to calculate the emission from the compound nucleus, with a full conservation of energy, spin and parity. Therefor, the cross sections $\sigma_{ijk}(E_{\rm n})$ can be obtained with the phenomenological spherical optical potential.

3 Calculation results

In terms of the formula (1), the partial kerma coefficients for alpha, protons, deuteron, tritium, ^{3}He and ^{6}Li have been calculated and shown in Fig. 1. One can see that the calculations (solid line) of this work are greatly in agreement with the experimental data and the extrapolated data which are experimental in the sense that no theoretical concept is used in their determination[13]. It is worth to note that the experimental data (open triangle)[14] at 27.4 MeV are not corrected for the contributions from the low-energy cuts in the measured spectra[13]. Because of the large alpha-particle emission cross sections, its kerma coefficients is bigger than others as shown in Fig. 1. We also compare with the calculated results(dash line) derived from the GNASH code by Chadwick et al in the 20—30 MeV incident neutron energy region[15].

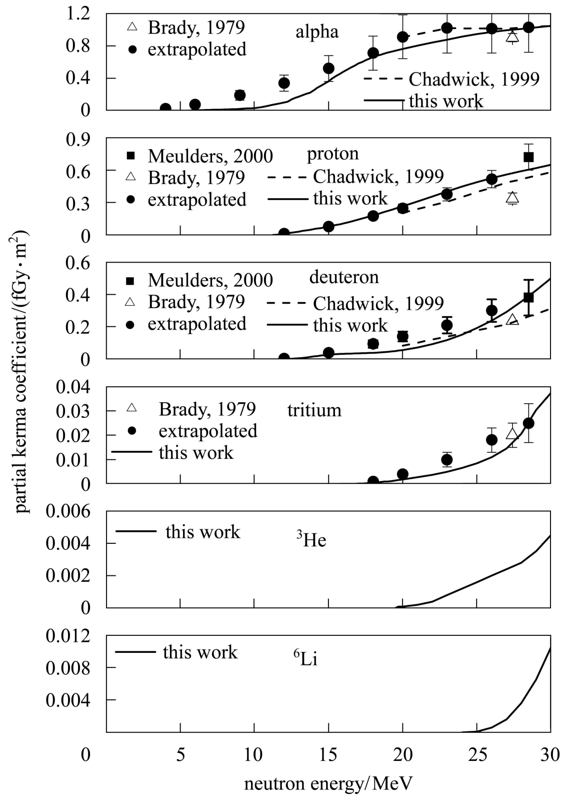

Fig. 1. Calculated partial kerma coefficients of this work for n+^{16}O reaction.

For neutron induced light nucleus reactions, the elastic scattering cross sections at low neutron energies have some peaks, which indicate their specific structures. However, the optical model calculation can obtain a smooth curve only. So, in the present work, the elastic cross section and their 1st Legendre coefficients $f_1^{m_1}(c)$ were derived from ENDF/B-VIIb.3. The calculated elastic recoil kerma coefficients of this work are shown as solid line in Fig. 2. The results are in good agreement with the experimental data, which are measured by Meulders et al[13] and by Borker et al[16]. In Fig. 2, we also give the theoretical results of alpha, proton and deuteron (dash line) in the 20—30 MeV incident neutron energy region[15].

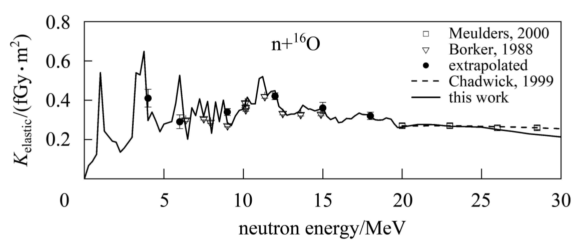

Fig. 2. The calculated elastic recoil kerma coefficients of this work for n+^{16}O reaction.

The calculated total kerma coefficients of this work (solid line) are compared with the experimental data and the evaluated results[15] (dash line), as shown in the Fig. 3. The experimental data (full square)[17] are compiled by Broeres et al. The data (open square, open dot, open triangle)[18] are derived from different oxides, and the residual data (full dot)[13] are measured by Meulders et al. Using the elastic cross sections and the 1st Legendre coefficients of ENDF/B-VIIb.3, we can reproduce the structural curves of the elastic recoil kerma coefficients below 30 MeV and the total kerma coefficients in the lower energy region. However, the present work underestimates the total kerma coefficients at about 6—20 MeV neutron region, and overestimates them above 20 MeV. The evaluated results[15] show the opposite behavior in the above two regions. Below 20 MeV, Chadwick et al use the NJOY data processing code to obtain the evaluation from existing ENDF/B-VI. Above 20 MeV, the results are calculated with the GNASH code[15].

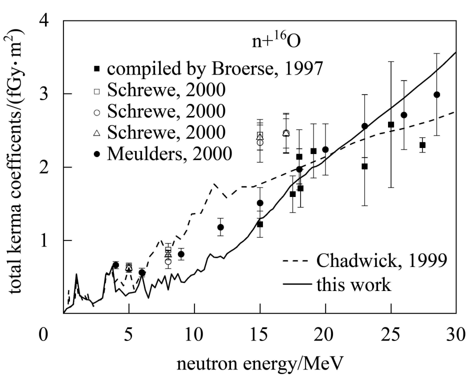

Fig. 3. The total kerma coefficients calculated in this paper for oxygen are compared with the experimental data and the evaluated results.

In terms of the formula (1), the total kerma coefficients are the sum of all partial kerma coefficients, which include the contributions of all kinds of charged particles from different reaction channels. The partial kerma coefficients of different charged particles shown in Fig. 1 and the elastic recoil kerma coefficients shown in Fig. 2 are in good agreement with the experimental data, therefore we think that the discrepancies of the calculated total kerma coefficients with experimental data can be attributed to the inelastic scattering channel.

In the ENDF/B-VIIb3 library (this new version for Oxygen has some improvement on inelastic scattering over earlier versions, such as ENDF/B-VI and so on.), the inelastic reaction channel corresponding to gamma-emitting excited levels of ^{16}O include the 1st—5th, 9th, 10th excited levels and continuum state levels. The 6th—8th excited levels are omitted because they decay primarily by alpha particle emission, therefore those data are included in the (n, α) channel. The cross sections for continuum state levels performed by GNASH[15] from threshold to 30 MeV, are adjusted such that the difference between total and nonelastic cross sections agrees with elastic cross section measurements. In this work, the pure inelastic scattering channel corresponding to gamma-emitting excited levels include the 1st—5th, 9th, 10th and 12th excited levels. The 6th—8th, 11th, 13th—17th excited levels can emit alphas, therefore their contributions are included in (n, nα) channel. The 18th excited level can emit protons and contributes to the (n, np) channel. The 19th and higher excited levels can emit several light particles, including neutron, proton, alpha, deuton and tritium, so their contribution belong to (n, 2n), (n, np), (n, nd), (n, nt) and (n, nα) channels, respectively. The discrepancies between the model calculations and the experimental data indicate that the processing way of inelastic scattering must be improved further in detail.

Figure 4 shows the contribution of the different charged particle partial kerma coefficients at the different incident neutron energies. The elastic recoil kerma coefficients (dash line) are dominant to the total kerma coefficients (solid line) in the low incident neutron energy region. However, the alpha-particle (dot line) and proton (dot-dash line) kerma coefficients are dominant in the higher energy region. The deuteron kerma coefficients (dash-dot-dot line) obviously increase for energies higher than 15 MeV. The results for tritium, ^{3}He and ^{6}Li are provided too in Fig. 4. Although the contributions of tritium, ^{3}He and ^{6}Li to the total kerma coefficients are small, they increase with incident neutron energy as shown in Fig. 4.

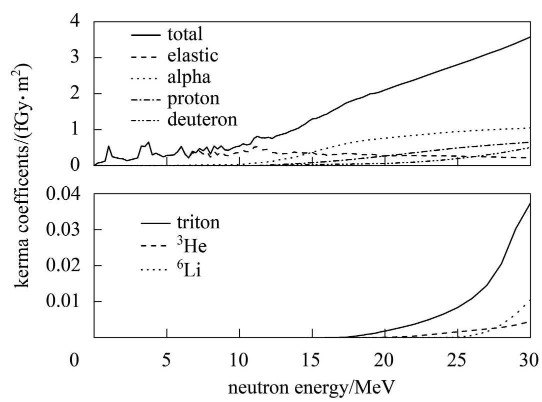

Fig. 4. The contribution of the different charged particle partial kerma coefficients versus the neutron energies.

4 Summary

A new kerma coefficient calculation formula, based on the light nuclear reaction model, has been determined. The emitted particle energies in different reaction channels are presented and the energy balance is strictly fulfilled. In terms of the new formulae, the results of the charged-particle and the elastic recoil partial kerma coefficients agree fairly well with the experimental data. The results of the total kerma coefficients have some discrepancies with the experimental data. We think that the discrepancies can be attributed to the different ways of processing inelastic scattering channel, so we will attempt to improve them in the future. At the same time, we will continue to study the kerma coefficients of other light nuclear elements in the future.

References

1 Reinhard W S. Radiation Research, 2001, **156**(2): 223—224
2 MacFarlane R E, Muir D W. Los Alamos National Laboratory report, 1994, LA-12740-M
3 LI Zhang, Abdou M A. Fusion Engineering and Design, 1997, **36**: 479—503
4 ZHANG Jing-Shang, HAN Yin-Lu, CAO Li-Gang. Nuclear Science and Engineering, 1999, **133**: 218—234
5 ZHANG Jing-Shang, HAN Yin-Lu. Commun. Theor. Phys., 2001, **36**: 437—442
6 ZHANG Jing-Shang, HAN Yin-Lu. Commun. Theor. Phys., 2002, **37**: 465—474
7 ZHANG Jing-Shang. Commun. Theor. Phys., 2003, **39**: 433—438
8 ZHANG Jing-Shang. Commun. Theor. Phys., 2003, **39**: 83—88
9 SUN Xiao-Jun, DUAN Jun-Feng, WANG Ji-Min et al. Commun. Theor. Phys., 2007, **48**: 534—540
10 YAN Yun-Liang, DUAN Jun-Feng, SUN Xiao-Jun et al. Commun. Theor. Phys., 2005, **44**: 128—132
11 DUAN Jun-Feng, YAN Yun-Liang, WANG Ji-Min et al. Commun. Theor. Phys., 2005, **44**: 701—706
12 DUAN Jun-Feng, YAN Yun-Liang, SUN Xiao-Jun et al. Commun. Theor. Phys., 2007, **47**: 102—106
13 Meulders J P, Benck S, Slypen I et al. Med. Phys., 2000, **27**: 2541—2559
14 Brady F P et al. Final report to the National Cancer Institute, 1979, Grant No.**IR01**, CA16261
15 Chadwick M B, Barschall H H, Caswell R S et al. Med. Phys., 1999, **26**: 974—997
16 Borker G, Bottger R, Brede et al. Radiat. Prot. Dosim., 1988, **23**: 23—26
17 Broeres J J et al. Nuclear data for neutron therapy: Status and future needs, IAEA-TECDOC-992, 1997
18 Schrewe U J, Newhauser W D, Brede H J et al. Phys. Med. Biol., 2000, **45**: 651—683